Coupled-resonator-induced-transparency concept for wavelength routing applications

M. Mancinelli,* R. Guider, P. Bettotti, M. Masi, M. R. Vanacharla, and L. Pavesi

Nanoscience Laboratory, Department of Physics, University of Trento, Povo 38100, Trento, Italy

*mancinelli@science.unitn.it

Abstract: The presence of *coupled resonators induced transparency* (CRIT) effects in *side-coupled integrated spaced sequence of resonators* (SCISSOR) of different radii has been studied. By controlling the rings radii and their center to center distance, it is possible to form transmission channels within the SCISSOR stop-band. Two different methods to exploit the CRIT effect in add/drop filters are proposed. Their performances, e. g. linewidth, crosstalk and losses, are examined also for random variations in the structural parameters. Finally, few examples of high performances mux/demux structures and 2×2 routers based on these modified SCISSOR are presented. CRIT based SCISSOR optical devices are particularly promising for ultra-dense wavelength division multiplexing applications.

© 2011 Optical Society of America

OCIS codes: (130.3120) Integrated optics devices; (230.4555) Coupled resonators; (060.4265) Networks, wavelength routing; (060.1155) All-optical network.

References and links

1. B. E. Little, S. T. Chu, J. V. Hryniewicz, and P. P. Absil, "Filter synthesis for periodically coupled microring resonators," Opt. Lett. **25,** 344–346 (2000).
2. Y. Xu, Y. Li, R. K. Lee, and A. Yariv, "Scattering-theory analysis of waveguide-resonator coupling," Phys. Rev. E **62,** 7389–7404 (2000).
3. D. D. Smith, Chang H., K. A. Fuller, A. T. Rosenberger, and R. W. Boyd, "Coupled-resonator-induced transparency," Phys. Rev. A **69,** 063804 (2004).
4. Q. Xu, S. Sandhu, M. L. Povinelli, J. Shakya, S. Fan, and M. Lipson, "Experimental realization of an on-chip all-optical analogue to electromagnetically induced transparency," Phys. Rev. Lett. **96,** 123901 (2006).
5. K. Totsuka, N. Kobayashi, and M. Tomita, "Slow light in coupled-resonator-induced transparency," Phys. Rev. Lett. **98,** 213904 (2007).
6. B. Maes, P. Bienstman, and R. Baets, "Switching in coupled nonlinear photonic-crystal resonators," J. Opt. Soc. Am. B **22,** 1778–1784 (2005).
7. R. W. Boyd and D. J. Gauthier, "Transparency on an optical chip," Nature (London) **441,** 701–702 (2006).
8. M. Mancinelli, R. Guider, M. Masi, P. Bettotti, M. R. Vanacharla, J. M. Fedeli, and L. Pavesi, "Optical characterization of a SCISSOR device," submitted to Optics Express.
9. Y. A. Vlasov and S. J. McNab, "Losses in single-mode silicon-on-insulator strip waveguides and bends," Opt. Express **12,** 1622–1631 (2004).
10. B. E. Little and J. Laine, "Surface-roughness-induced contradirectional coupling in ring and disk resonators," Opt. Lett. **22,** 4–6 (1997).
11. S. Cho and R. Soref, "Apodized SCISSORs for filtering and switching," Opt. Express **16,** 19078–19090 (2008).
12. C. A. Brackett , "Dense wavelength division multiplexing networks: principles and applications," IEEE J. Sel. Areas Commun. **8,** 948–964 (1990).
13. M. Masi, R. Orobtchouk, G. F. Fan, and L. Pavesi, "Towards realistic modeling of ultra-compact racetrack resonators," J. Lightwave Technol. **22,** 3233–3242 (2010).

#139924 - $15.00 USD Received 20 Dec 2010; revised 4 Feb 2011; accepted 1 Apr 2011; published 9 Jun 2011
(C) 2011 OSA

14. Q. Xu, J. Shakya, and M. Lipson, "Direct measurement of tunable optical delays on chip analogue to electromagnetically induced transparency," Opt. Express **14,** 6463–6468 (2006).
15. Z. Sheng, L. Liu, S. He, D. Van Thourhout, and R. Baets, "Silicon-on-insulator microring resonator for ultra dense WDM applications," in Proceedings of IEEE Conference on Group IV Photonics (IEEE, 2009), pp 122–124.

1. Introduction

Photonic devices based on coupled optical resonators present many novel effects [1, 2]. In particular, electromagnetically induced transparency (EIT)-like effects can occur in coupled optical resonators due to coherent interference [3]. This effect was recently demonstrated in side coupled integrated spaced sequence of resonator (SCISSOR) composed by two microresonators [4], and can lead to a high variety of applications in advanced photonic devices [5, 6], and in integrated all-optical chips [7]. SCISSORs have a rich optical phenomenology due to the interplay between the coherent feedback of all the rings when the wavelength of the signal satisfies a Bragg-like condition and the resonant behavior of the rings which form a resonator stop-band [8, 11].

The coupled resonators induced transparency (CRIT) effect in a SCISSOR structure occurs when the input signal has a wavelength which is resonant with two or more rings. In this case the signal is coupled to the side waveguide through two or more rings. If this light interferes constructively, it is coupled back in the input waveguide and CRIT is observed. Constructive interference is achieved if the round-trip phase between two or more rings is a multiple of 2π. This condition is satisfied when the center to center distance L_c between adjacent rings (coherence length), is a multiple of πR, where R is the radius of the rings [4]. If the CRIT condition is satisfied, the transmission spectrum of the SCISSOR exhibits a very narrow transparency peak inside the resonator stop-band.

In this work we study the CRIT effect in SCISSOR devices in order to demonstrate a novel way to exploit it for signal routing. A new design will be presented where modified SCISSOR structures are used to control the spectral position of the CRIT resonance. The coherent interference among the resonators will be carefully detailed. Two methods to control the CRIT, which are based on different principles, will be studied. In addition, we will consider the consequence of the limited resolution in current lithographic processes on the router performances, in particular on the insertion losses and crosstalk.

All the results are obtained through numerical simulations based on a Transfer Matrix algorithm. The methodology is quite general and it is carefully described in Ref. [8]. The input parameters to the simulations are the geometry of the SCISSOR (ring radii, coherence length and ring number), the effective index of the waveguides and the coupling coefficient between the waveguide and the ring. Polarization and waveguide to ring gap distance are then determined to get that specific coupling coefficient with that particular effective index of the mode. The effective index used in simulations is obtained and reported in Table 1 by using a mode solver to simulate a SCISSOR device fabricated with the following characteristics [8]: silicon on insulator (SOI) waveguide (waveguide width $500\,nm$, waveguide height $220\,nm$, buried oxide thickness $1\,\mu m$) with ring resonators of radius $R = 6.75\,\mu m$, $L_c = 21\mu m$ and waveguide to ring gap $300\,nm$. Table 1 gives the simulation code parameters.

Table 1. Optical parameters used in the transfer matrix (TMM) simulations.

Wavelength λ (nm)	Effective Index n_{eff}	Coupling Coefficient κ^2	Round Trip Loss $\alpha\,(dB/90^\circ)$
From 1540 To 1550	$1.718 - 1.2 \times 10^{-3}(\lambda - 1540)$	From 10% To 80%	0, 0.006 Or 0.013

#139924 - $15.00 USD Received 20 Dec 2010; revised 4 Feb 2011; accepted 1 Apr 2011; published 9 Jun 2011
(C) 2011 OSA

2. Design of the structure

2.1. Fundamental

Figure 1(a) reports the *new* SCISSOR design which is composed by 7 resonators with different radii. The fourth resonator has a radius R, while the others have either decreasing or increasing radii. Each resonator differs from its neighbor by ΔR (detuning). All the resonators are coupled to the input and drop waveguides with the same coupling coefficient. The difference in radii between nearby resonators leads to a spectral shift of the single ring resonance and creates the condition for the creation of CRIT [4]. Indeed, if the two rings have the same radius, the signal is channelled into the drop waveguide by the first ring. In this case, no signal reaches the second ring preventing the formation of the coherent feedback which yields the CRIT. One needs to slightly detune ($\Delta R \neq 0$) the resonances so that enough signal reaches the second ring allowing a significant coherent feedback. The detuning, on the other hand, must be small enough in order to keep the spectral overlap of two adjacent ring resonances.

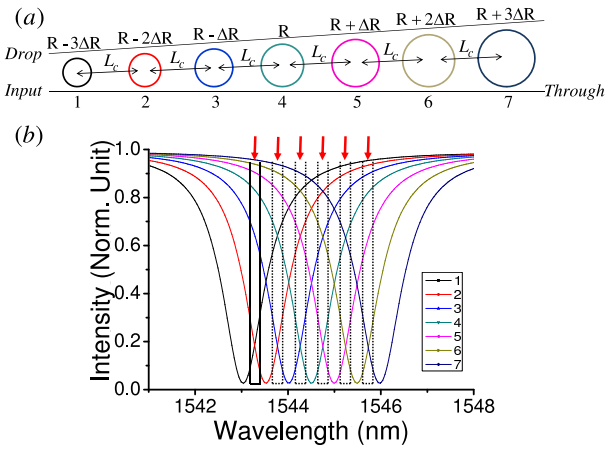

Fig. 1. (a) Schema of the new SCISSOR for 7 ring resonators: R represents the radius of the central resonator, ΔR the detuning and L_c the coherence length. The resonators are labelled from 1 to 7 starting from the left. (b) Simulated spectra of the through signal for each resonator. The black rectangles and red arrows correspond to the possible wavelength where CRIT might occur.

Having different radii, each resonator is characterized by a different resonant wavelength. If we consider the through signal when all the resonators are acting independently, i. e. are isolated, we find the sequence of spectra shown in Fig. 1(b). However in the SCISSOR structure, the single resonators are coupled through the drop waveguide: it is the choice of the coupling length which determines the coherent interaction between the signal resonant to the various resonators. If L_c satisfies the constructive interference condition we have CRIT. If not, we do not have any through signal. This is demonstrated in Fig. 2 where we plot with the black line the through signal when the condition for destructive interference is satisfied and with the red line the through signal when the condition for constructive interference is satisfied. Note that since the radii of the rings are all different, L_c is different for each pair of rings. The coherence length is obtained using the mean radius between the two resonators:

$$R_m(n) = \frac{R(n) + R(n+1)}{2},$$

#139924 - $15.00 USD Received 20 Dec 2010; revised 4 Feb 2011; accepted 1 Apr 2011; published 9 Jun 2011
(C) 2011 OSA

where $R_m(n)$ is the mean radius of the n_{th} pair of resonators and $R(n)$ is the radius of the n_{th} ring. Then, if $L_c(n)$ is the distance of the n_{th} pair of rings, $L_c(n) = \pi R_m(n)$ is the condition which has to be satisfied for constructive interference for that ring pair and $L_c(n) = \frac{3}{2}\pi R_m(n)$ for destructive interference.

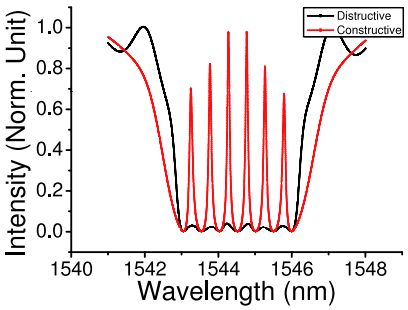

Fig. 2. Example of the through port response for a CRITAD made with 7 ring resonators in which all pairs are in constructive (red line) and destructive (black line) interference.

In this case we have a flat stop-band which is typical of a sequence of rings. Note that the spectral position and the presence of each one of these CRIT peaks is carefully controlled by the choice of ring radii and of coherence lengths in this new tapered design: each single CRIT peak forms only via the coupling of a single pair of resonators. This avoids the random formation of CRIT peaks which might occur in more complex situations where more than two rings might be coupled [8].

Since only one pair generates a single CRIT resonance, the maximum number of available CRIT resonances for N resonators will be N-1. In addition, in the proposed structure, all pairs are formed by adjacent rings to minimize the effective length of the *cavity* that generates the CRIT.

Figure 3 compares an add-drop filter (named RAD) based on a single resonator with an add-drop filter made with the proposed SCISSOR design (named CRITAD). The design parameters are the same in the two case, i. e. the same average ring radius, coupling coefficients, losses etc. Note that, for the CRITAD, the CRIT condition has been imposed only on one pair of rings in order to have a single CRIT resonance. In Fig. 3, the through signal is reported in the two cases.

It is interesting to note that:

- the RAD has a blocking characteristic when in resonance, while the CRITAD is transparent;
- even if the Q factor of individual rings are the same, CRITAD has much narrower linewidth ($\sim 0.1\,nm$) if compared with RAD ($2\,nm$).
- the series of coupled rings in the CRITAD form a large stop-band whose width can be controlled by the number and sizes of the rings;
- the single CRIT resonance can be understood as the single channel in the add-drop while the other wavelengths within the stop-band are channelled into the drop ports.

Finally, let us note that the spectral characteristics of the single CRIT channel depend on the propagation losses, the coupling coefficient κ^2 , the coherence length and on the detuning of the resonances (Fig. 1) [4]. In particular, the insertion losses (losses of the signal in resonance

#139924 - $15.00 USD Received 20 Dec 2010; revised 4 Feb 2011; accepted 1 Apr 2011; published 9 Jun 2011
(C) 2011 OSA

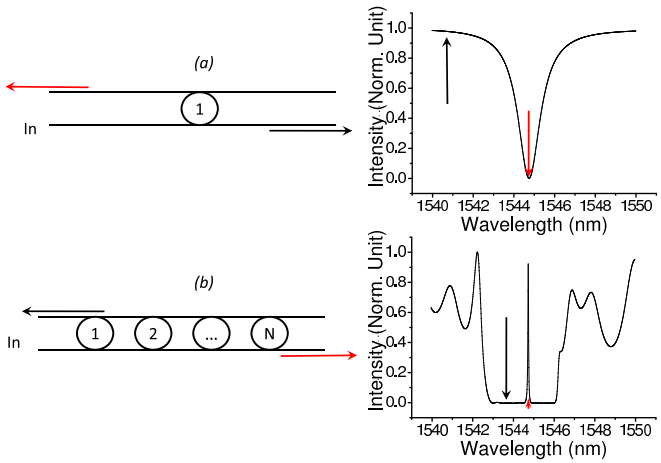

Fig. 3. Schematic representation of the two types of structure, RAD (structure a) and CRITAD (structure b) with the wavelength response of the through signal in equal simulation conditions. The black (red) arrow represent the passive (active) state. The CRITAD is composed by 7 resonators in which the active couple is the fourth (not shown in the schema).

with the CRIT channel) are mainly due to the radiative losses of the cavities that are related to material type and the fabrication imperfections (surface roughness).

2.2. *Control of the interference*

Consider the case with all resonators in destructive interference condition ($L_c = 3/2\,\pi R_m$) and "open" a CRIT channel by putting in constructive interference only one pair of resonators ($L_c = \pi R_m$). This method will be called *local* method.

Figure 4 shows how to create two different transmission channels in two different CRITAD by using the *local* method. We start from a basic block (blue line) made by 3 resonators in destructive coherent feedback condition. The effect of changing the phase from destructive to constructive interference of a single pair allows the creation of one CRIT channel (Fig. 4 for channel A (red line) and channel B (black line)).

Another method to control the positions of the transmission channel is to change the spectral position of the Bragg stop-band formed by the coherent overlap of the reflection of the various rings. This can be done by changing the coherence length L_c among the various rings. In fact, the *Bragg* stop-band is centered at the wavelength λ_b defined by:

$$\lambda_b = \frac{2L_c\, n_{eff}}{m_b},$$

where m_b is the order of the Bragg band and n_{eff} is the effective index of the optical mode in the waveguide [8]. This method will be called *Bragg* method.

In order to understand the *Bragg* method, we show in Fig. 5 (a) the schematic of the CRITAD and in Fig. 5 (b) a sketch of the through response for two different values of the Bragg stop-band determined by two different values of L_c. Note that also in this case the radii of the various rings differ by ΔR.

Within this method, to have a CRIT channel, the spectral position of the Bragg stop-band has to overlap with the CRIT condition of a pair of neighboring rings, i. e. $\lambda_b = 2\pi R_m\, n_{eff}/m_b$. This

#139924 - $15.00 USD Received 20 Dec 2010; revised 4 Feb 2011; accepted 1 Apr 2011; published 9 Jun 2011
(C) 2011 OSA

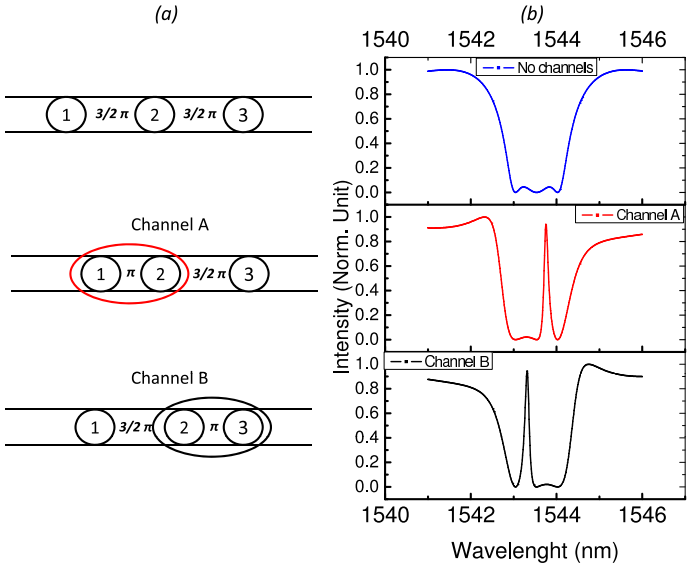

Fig. 4. Schema of the 3 rings *local* CRITAD structure (a) and spectrum of the through signal (b) for: (Top) destructive interference, (Middle) constructive interference of the first pair, (Bottom) constructive interference of the second pair. The radius of the rings differs by ΔR .

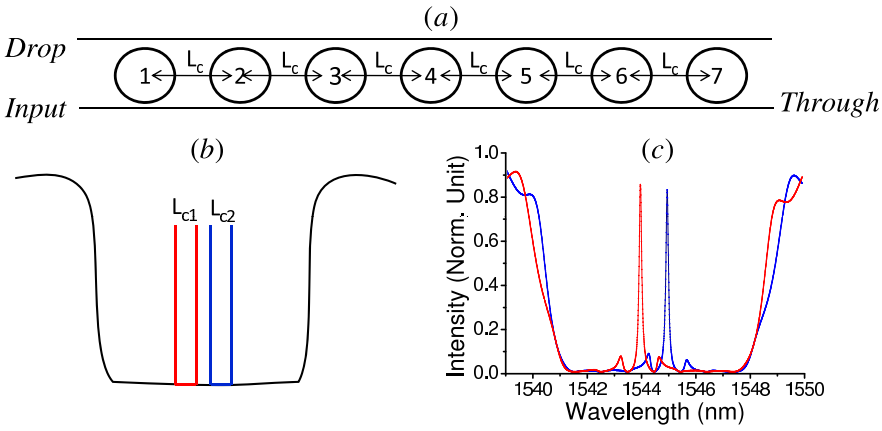

Fig. 5. Schema of the 7 rings *Bragg* CRITAD structure (a) and spectra of the through signal for different coherent distances L_{c1} (red) and L_{c2} (blu). (b) Schematic view of the position of the Bragg band inside the stop-band and (c) spectral response of the through port for the 2 different L_c . The radius of all rings differs by ΔR .

#139924 - $15.00 USD Received 20 Dec 2010; revised 4 Feb 2011; accepted 1 Apr 2011; published 9 Jun 2011
(C) 2011 OSA

is demonstrated in Fig. $5(c)$ where the through signal is reported for two SCISSOR structures which differ only for L_c.

3. Performances of the new SCISSOR design as an add/dropp filter

3.1. Performance of the structures

We compare the two methods to form a CRITAD by computing the bandwidth (defined as the resoannce linewidth at -3 dB in GHz), the channel losses (defined as the intensity in dB of the through signal when the wavelength is equal to the channel wavelength and the input intensity is 1) and the crosstalk (defined as the difference between the channel losses and the intensity in dB of the through signal when the wavelength is different from the channel (resonance) wavelength).

For both cases, the schemes of the structures are similar to the one shown in Fig. 1. Both have 7 rings of radius $R = 6.75\,\mu m$, and for each method, we used two values of ΔR : 5 and $10\,nm$. The coherence length L_c is equal to πR_m or $3/2\,\pi R_m$ depending on the design. Since it was reported in sub-micrometer SOI waveguides a bending loss of $0.006\,dB/90^o$ for a bending radius of $5\mu m$ which translates into a propagation losses of $6\,dB/cm$ [9], we vary in our simulations the propagation losses: 0, 6 and $12\,dB/cm$. Since in the microring resonator the coupling section (the section of the bus waveguide coupled evanescently with the resonator) is very short, almost punctiform, we have neglected the coupling losses. In the case of a racetrack resonator the coupling losses will become larger since the coupling section is longer (for racetrack with a coupling section of $10\mu m$ the coupling losses are of the order of $0.1dB$) [13].

In addition, we changed also the bandwidth of the CRIT channel, which is mainly controlled by the coupling coefficient (defined as the percentage of the optical field which is coupled into the ring resonator). This is shown in Fig. 7(a). The over-coupling regime ($\kappa^2 > r^2$ where r^2 is the *roughness-induced reflection*) allows to avoid the problem of the mode splitting induced by surface-roughness that becomes critical when using resonators in the under-coupling regime [10]. Values of coupling coefficient from 10% (wider gap width) to 50% (narrower gap width) were used for the $\Delta R = 5\,nm$ design and from 20% (wider gap width) to 80% (narrower gap width) for the $\Delta R = 10\,nm$ design.

Figure 6 reports the values of channel losses and crosstalk as a function of the channel bandwidth for different values of the bending losses. Figures $6(a)$ and $6(b)$ refer to the *local* method for two different values of ΔR. Figures $6(c)$ and $6(d)$ refer to a structure designed by using the *Bragg* method for two different values of ΔR.

We found that:

1. if the losses are zero, both methods yield negligible channel losses which are independent on the bandwidth;
2. if the losses are different from zero, the channel losses depend on the bandwidth;
3. the dependence on the channel losses to the bandwidth is stronger for the *local* than the *Bragg* method;
4. the bending losses limit the range of bandwidts where negligible channel losses exist;
5. the cross talk is larger for the *Bragg* than for the *local* method;
6. the crosstalk depends only slightly on the losses;
7. once fixed the process (i. e. fixed the losses), both designs are able to achieve the same bandwidth;

#139924 - $15.00 USD Received 20 Dec 2010; revised 4 Feb 2011; accepted 1 Apr 2011; published 9 Jun 2011
(C) 2011 OSA

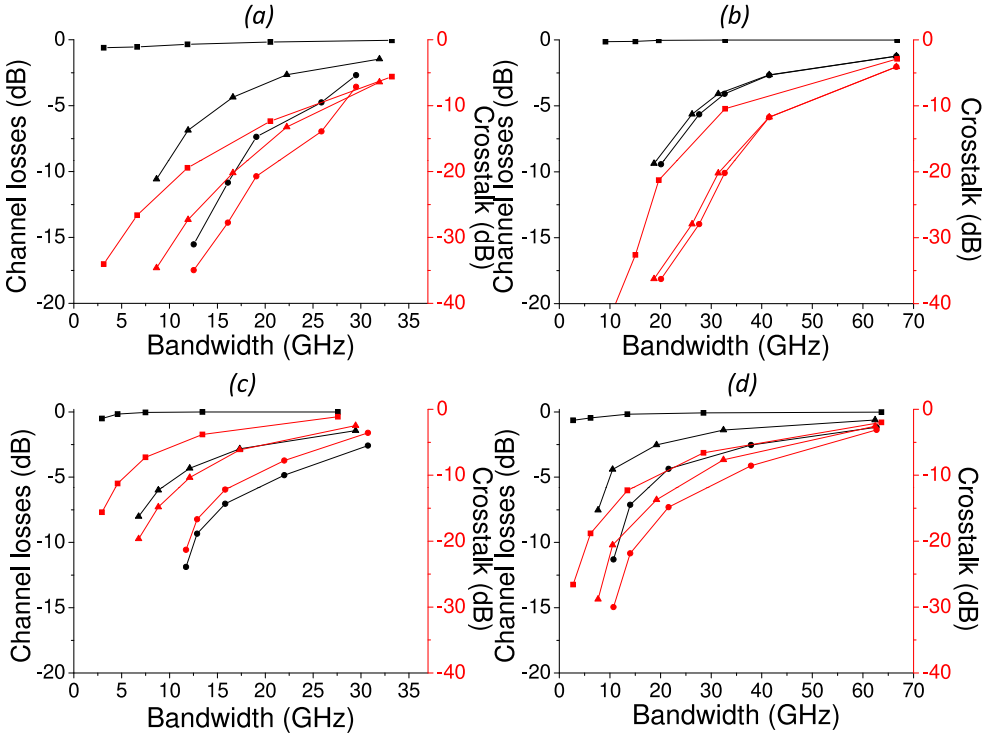

Fig. 6. Cross talk (red line) and losses (black line) of CRIT channel as a function of the bandwidth for 3 different values of the bend loss: $0dB/cm$ (Square), $6dB/cm$ (Triangle) and $12dB/cm$ (Circle). (a) Local method with $\Delta R = 5\,nm$ (b) Local method with $\Delta R = 10\,nm$ (c) Bragg method with $\Delta R = 5\,nm$. (d) Bragg method with $\Delta R = 10\,nm$. Other parameters are detailed in the text.

8. the *local* method shows a significant lower crosstalk but higher channel losses.

These results show that the choice of ΔR and coupling coefficients allow to adapt the performance of the CRITAD to the different routing requirements, e. g. for coarse wavelength division multiplexing (CWDM, bandwidth $> 500\,GHz$), dense WDM (DWDM, bandwidth $\sim 100\,GHz$) or ultra dense WDM (UDWDM, bandwidth $< 50\,GHz$) [12].

The crosstalk of CRITAD designed by the *Bragg* method can be decreased by increasing the number of rings in the SCISSOR while that of CRITAD designed by the *local* method is almost insensitive to the number of rings in the SCISSOR (see Fig. $7(b)$). This is due to the fact that an increased number of rings in the SCISSOR sharpens the Bragg stop-band. Hence, the crosstalk is decreased for the CRITAD designed by the *Bragg* method where the Brag stop-band rules its behavior.

A final comment is about the footprint of the CRITAD: for the same number of rings, the *local* method yields SCISSOR which are $1/3$ longer than SCISSOR obtained by the *Bragg* one, since in the *local* method the coherence length is $3/2\,\pi R_m$ instead of the πR_m length needed for the *Bragg* method.

#139924 - $15.00 USD Received 20 Dec 2010; revised 4 Feb 2011; accepted 1 Apr 2011; published 9 Jun 2011
(C) 2011 OSA

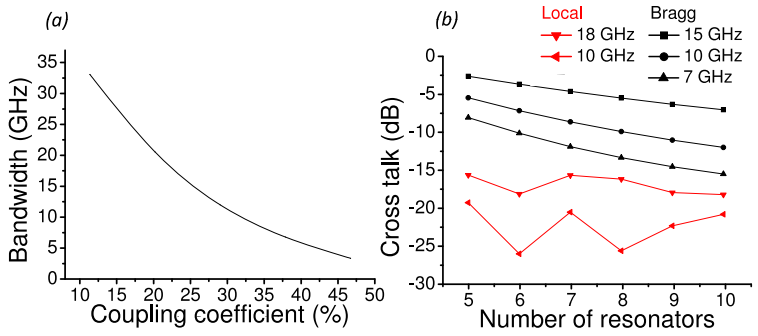

Fig. 7. (a) Bandwidth of a CRIT channel versus the coupling coefficient used in the simulation. These values are for the local method and a ΔR of $5\,nm$. (b) Crosstalk versus the number of rings that compose the CRITAD for different values of channel bandwidth (reported in the legend) and different design: (black) Bragg method, (red) local method. The losses were fixed to $6\,dB/cm$.

3.2. *Phase and group delay*

The very narrow bandwidth of the CRITAD is reflected in short pulse dispersion. This property can be used for slow light studies or for making delay lines [14]. Figure 8 reports the phase shift and the group delay for the through signal of a CRITAD. The phase shift was evaluated by the transfer matrix method while the group delay was computed via the dispersion of the phase shift:

$$\tau_g = \frac{d\phi}{d\omega},$$

where τ_g is the group delay, ϕ is the phase shift and $\omega = 2\pi c/\lambda$ is the frequency. The group delay is related to the group velocity ($v_g = L/\tau_g$, where L is the SCISSOR length) and, in turns, to the temporal broadening that a pulsed signal suffers while being transmitted by the CRITAD to the through port. Therefore, τ_g limits the data rate that can be sent in the CRITAD.

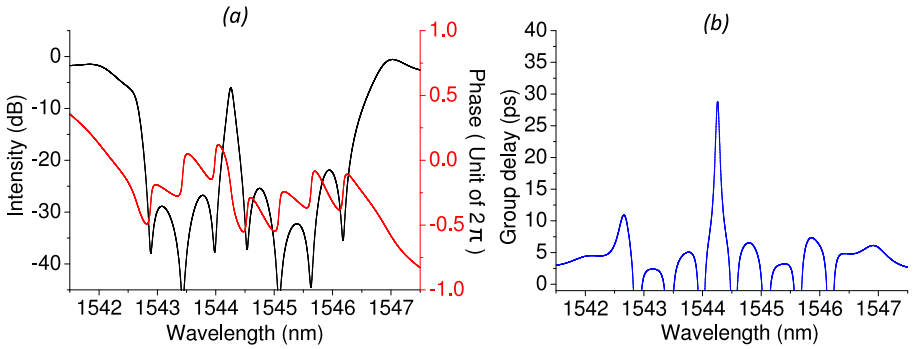

Fig. 8. (a) Spectral response of the through signal for a CRITAD with the *local* design and a $\Delta R = 5\,nm$: signal intensity (black) and signal phase shift (red). (b) Group delay (blue) of the through signal.

Figure 8 shows the results for a CRITAD designed by the *local* method with a 7 ring SCISSOR where the pairing occurs between the 3rd and 4th rings (Fig. 2). The various parameters

#139924 - $15.00 USD Received 20 Dec 2010; revised 4 Feb 2011; accepted 1 Apr 2011; published 9 Jun 2011
(C) 2011 OSA

are: bend losses of $6\,dB/cm$, coupling coefficient of 25% and $\Delta R = 5\,nm$. It is observed that the phase changes by $0.8(2\pi)$ across the CRIT resonance, that the maximum τ_g is $28\,ps$ with a bandwidth of $12\,GHz$. This value of group delay limits the bit rate to $30\,Gb/s$. If we increase the bandwidth to $22\,GHz$ by using a coupling coefficient of 55% and a $\Delta R = 10\,nm$ the maximum τ_g decreases to $17\,ps$, which in turn means a maximum bit rate of $50\,Gb/s$.

3.3. Robustness to fabrication random errors

The CRITAD is a building block which needs to be repeated for multi-channel routers. The fabrication processing errors during the manufacture of the router can become relevant. It is therefore necessary to look at their influence on the proposed designs. To study this effect, we added random lengths to the nominal radius R and coherence length L_c of each ring and ring spacing in the SCISSOR. These random lengths are normally distributed with zero mean and with a standard deviation σ of the order of few nanometers. Note that in processing, the length specification errors are usually given as 3 σ from the average. We define the channel width (bandwidth) as the FWHM of the resonance, and we center the channel at the CRIT resonance wavelength of the ideal case (no errors).

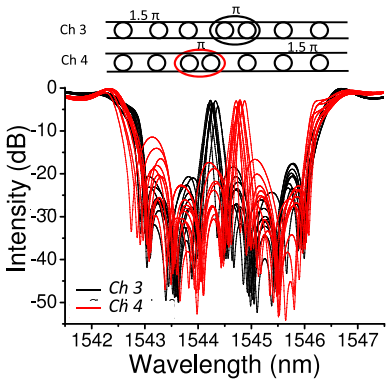

Fig. 9. Through port response for 2 CRITAD devices made with local method: (black) 3th channel open, (red) 4 th channel open. The multiple red (black) curves represent the effect of $3\sigma = 3\,nm$ fabrication error. The parameters used are $R = 6.75\mu m$, coupling coefficient 20%, $L_c = 3/2\pi R_m$.

Table 2. Table showing the average value for channel losses and crosstalk with relative standard deviation for 3 different values of structural errors, $3, 6, 9\,nm$, and two ΔR, 5 and $10\,nm$. The parameters obtained with $0\,nm$ of error represent the values obtained from the ideal structures. The parameters were obtained from a sample of 100 CRITAD.

Error (3σ)	Bandwidth $11\,GHz$ ($\Delta R = 5\,nm$)		Bandwidth $22\,GHz$ ($\Delta R = 10\,nm$)	
(nm)	Losses (dB)	Crosstalk (dB)	Losses (dB)	Crosstalk (dB)
0	-04.44 ± 00.00	-19.56 ± 00.00	-01.61 ± 00.00	-18.56 ± 00.00
3	-06.45 ± 03.77	-17.80 ± 06.74	-01.70 ± 00.41	-18.59 ± 02.43
6	-12.48 ± 07.98	-12.86 ± 12.11	-02.37 ± 01.74	-19.32 ± 05.98
9	-13.39 ± 09.48	-13.18 ± 13.90	-04.50 ± 04.86	-16.50 ± 09.45

Figure 9 shows the results of various simulations where the random errors have a standard deviation of $1\,nm$. Here two CRITAD with two different channels and ΔR of $5\,nm$ were simulated.

#139924 - $15.00 USD Received 20 Dec 2010; revised 4 Feb 2011; accepted 1 Apr 2011; published 9 Jun 2011
(C) 2011 OSA

Unwanted peaks or spectral shifts caused by the pairing of other rings are avoided by imposing the condition of destructive interference between the resonators. In fact, to have a paring the coherence length between adjacent rings should change by $1/2\pi R \simeq 10\mu m$. If the coherence condition would have not been imposed, random pairing of rings would have occurred and unwanted CRIT resonances would have appeared in the stop-band, as experimentally observed in [8].

A summary of a statistical analysis over 100 realizations of CRITAD with different randomness and various ΔR is reported in Tab. 2. Here we show the losses and crosstalk induced by fabrication errors. By increasing the fabrication errors we note an increase in the channel losses due to small random fluctuations of the CRIT resonance: the error value at which the losses increase by 3 dB with respect to the ideal case is the error at which the CRIT resonance statistically shifts more than the defined channel bandwidth.

In addition, the channels are completely smeared out when the losses and crosstalk have the same value.

A good robustness to fabrication errors of $3\,nm$ is observed for both bandwidths. The $22\,GHz$ one shows a very good strength up to $9\,nm$ of error. The performances deteriorate for larger fabrication errors, especially when small bandwidths are required. These simulations show that the application of these devices in UDWDM requires an extremely accurate and stable processing.

4. CRIT based passive multiplexer/demultiplexer

The possibility given by the CRITAD to have multiple narrow channels inside the same stop-band suggests to look for applications in Wavelength Division Multiplexing. Here, we discuss a design which yields a compact mux/demux.

Figure $10(a)$ shows a schema of a $4\times 1/1\times 4$ mux/demux. This structure consists of a combination of 4 cascaded CRITAD. Each SCISSOR is designed to have only one CRIT channel by pairing only two resonators in constructive phase condition ($L_c = \pi R_m$) while all the others are coupled in destructive phase conditions ($L_c = \frac{3}{2}\pi R_m$). Figure $10(b)$ shows the transmitted signal out of the four output ports when no propagation and bending losses are considered. Figure $10(b)$ shows the same when 6 dB/cm of propagation and bending losses are assumed. When the input signal has a wavelength within the stop-band but different than the CRIT condition for the various SCISSOR, it crosses all the SCISSOR. On the contrary, when the input signal has a wavelength which satisfies the CRIT condition for anyone of the 1-4 channels it is transmitted in the corresponding output channel. Clearly, the structure can also work as a multiplexer if the four outputs are used as inputs: in this case four different wavelengths within the SCISSOR stop-band are channelled into the single output waveguide (from right to the left in the figure).

Note that the channels have similar insertion losses (channels balanced) and also that the effect of sizeable propagation losses are to slightly increase the crosstalk ($< 20\,dB$) while keeping acceptable insertion losses of $7-8\,dB$. These figures are obtained for channel separations $< 30\,GHz$ and a channel bandwidth of $12\,GHz$. If larger bandwidths are acceptable, (e. g. $38\,GHz$ which is obtained by a $\Delta R = 10\,nm$), similar crosstalk values are obtained but the channel losses decrease to about $3\,dB$. It is straigthforward to expand this design to a $1\times N$ mux/demux by increasing the number of rings and SCISSOR.

Finally, it is also possible to turn on/off one channel, whitout disturbing the others, by changing locally the refractive index of a ring in the couple that does CRIT. Control of the ring refractive index, can be achived with an integrated heater or an integrated *p-n* junction. By modifying the refractive index, the CRIT condition is no longer met and the transmission channel vanishes in the SCISSOR stop-band [8].

#139924 - $15.00 USD Received 20 Dec 2010; revised 4 Feb 2011; accepted 1 Apr 2011; published 9 Jun 2011
(C) 2011 OSA

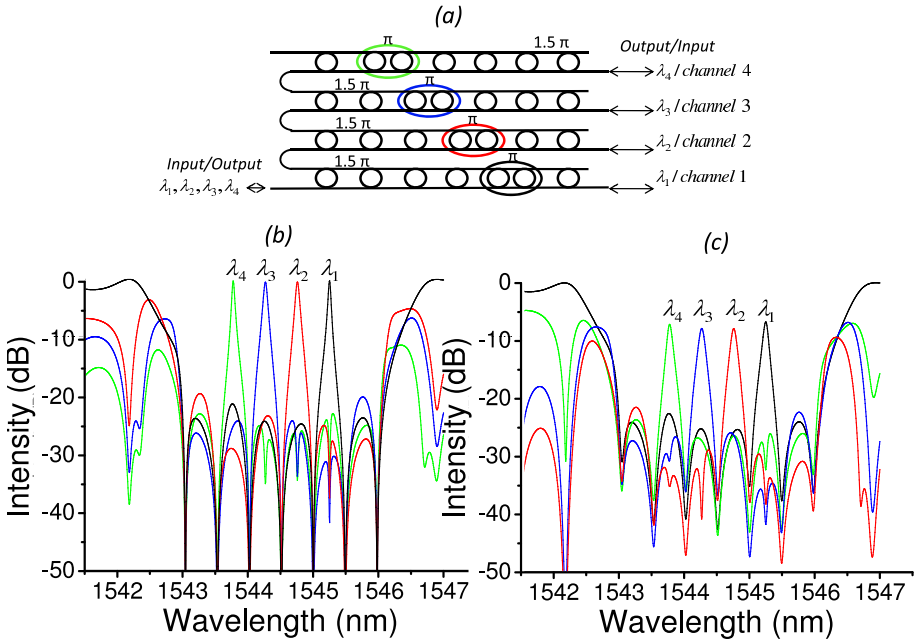

Fig. 10. (a) Schema representing a $4\times1(1\times4)$ multiplexer (demultiplexer) based on *local* method CRITAD, composed by 7 resonators, in which the colored circles identifies the pair that does CRIT and then creates a channel. (b) Simulated spectral response, without considering losses, of the 4 channels in which the colors are linked to the schema of the structure. (c) Simulated spectral response, considering losses of $6\,dB/cm$. The parameters used are $R=6.75\,\mu m$, $\Delta R=5\,nm$, coupling coefficient 23% .

5. CRIT 2×2 router

Another possible application of the proposed new SCISSOR design is the realization of a 2×2 router.

Table 3. Table of routing of the structure. The parameters used are $R=6.75\,\mu m$, $\Delta R=5\,nm$, coupling coefficient 23% and bend losses $6\,dB/cm$.

		Out			
		a	*b*	*c*	*d*
In	*a*	×	×	λ_2	λ_1
	b	×	×	λ_1	λ_2
	c	λ_2	λ_1	×	×
	d	λ_1	λ_2	×	×

To build a 2×2 bidirectional router one needs four SCISSOR, each couple of which has the same CRIT resonance. The four SCISSORS are arranged as in Fig. $11(a)$. Each SCISSOR is composed by 5 rings and, in this implementation, it is designed by using the *local* method. In the sketch, the SCISSORs which have the CRIT resonant on channel 1 (λ_1) are circled in black while the other two in resonance with channel 2 (λ_2) are circled in red. All the inputs *a, b, c, d* are bidirectional. For each input is associated only one output where the selection is

#139924 - $15.00 USD Received 20 Dec 2010; revised 4 Feb 2011; accepted 1 Apr 2011; published 9 Jun 2011
(C) 2011 OSA

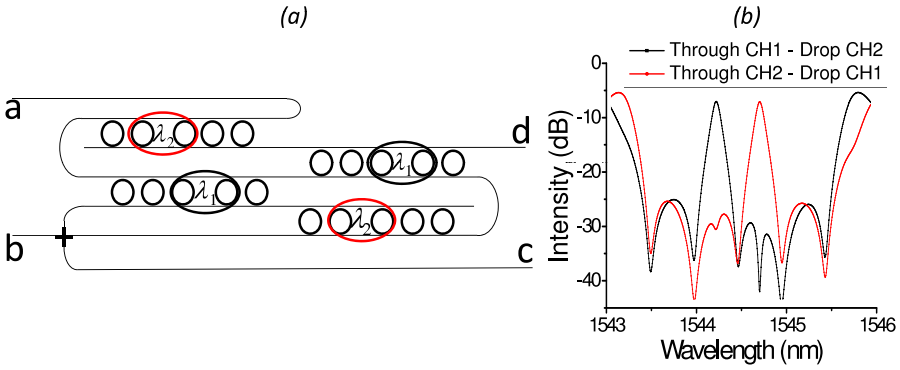

Fig. 11. (a) Schema representing a 2×2 router based on local method CRITAD, composed by 5 resonators, in which the colored circles identify the pair that does CRIT and then creates a channel. (b) The black (red) curve represents the simulated spectrum obtained with $\lambda_{1(2)}$ that passes through the transparency of SCISSOR $1(2)$ and the resonance of SCISSOR $2(1)$.

determined by the input signal wavelength. If the signal is injected at input *b* with a wavelength λ_1, it is dropped by the first SCISSOR it encounters and it is transmitted to output *c* by the next SCISSOR. Figure $11(b)$ shows the transmitted signal from port *a* and *b* to port *c* and *d* as a function of the wavelength. It is observed that only a specific wavelength entering in a given input port can be routed to a given output port.

The Table 3 shows the correspondence among the various inputs/outputs. This structure is bidirectional and antisymmetric with respect to a change of the inputs with the outputs. For the assumed parameters, it can handle signals of $12\,GHz$ bandwidth with channel losses of $7\,dB$ and crosstalk of less than $21\,dB$.

6. Conclusion

The presence of CRIT effects in SCISSOR can be exploited to realize new designs for high performance add/drop filters, multiplexers/demultiplexers and routers. These new types of structures are able to reach very narrow bandwidths, low crosstalk and insertion losses while keeping reasonable requirements on fabrication tolerance and design complexity. In particular, they show properties that makes them preferable to single ring resonator based scheme for UDWDM where the bandwidth requirements are so stringent that only rings in the under-coupled regime can satisfy. [15] These interesting properties are counterbalanced by the increased complexity of the proposed design which scales with the number N of channels according to $N \times (N-1)$. This, however, should not be a problem from a technological point of view since the robustness of the design to fabrication errors.

In addition, CRITAD allows:

1. to obtain an effective cavity length which is two times longer than the single ring cavity. This yields an higher Q-factor. Let us note, than in the CRITAD as in the RAD, the free spectral range (FSR) is determined by the ring dimension. In other words, the CRITAD compared to a RAD has larger Q-factors with the same FSR;

2. to achieve a sub-nanometer linewidth in the over-coupled regime while a ring resonator would have to work in an under-coupled regime to have the same linewidth. However, in

#139924 - $15.00 USD Received 20 Dec 2010; revised 4 Feb 2011; accepted 1 Apr 2011; published 9 Jun 2011
(C) 2011 OSA

this working regime, ring resonators are affected by a mode splitting nuisance which is induced by surface roughness [10, 15];

3. to define a transmission channel which is robust to fabrication errors. In the worst case of many fabrication errors, the CRITAD resonance is mainly depressed without moving out of the given channel;

4. to reduce the channel crosstalk since the sharp CRIT resonance lineshape cuts out the tails of the typical single lorentzian lineshape of the single ring resonance;

5. to get a structure which is more insensitive to fabrication errors than ring resonators. For a single ring with the same radius of those in our CRITAD, $3\,nm$ of variations in the radius (i.e. $\sigma = 1\,nm$) yields to a resonance shift of $0.22\,nm$. From Table 2, it is inferred that, for $\Delta R = 5\,nm$ and for $\sigma = 1\,nm$, the resonance of the CRITAD shifts by $0.09\,nm$ (the channel bandwidth), a value 2.5 times smaller than for a single ring.

The challenge left is the fabrication of these designs and the demonstration of their superior performances.

Acknowledgement

This work is supported by the European project FP7-ICT 216405 WADIMOS (wavelength division multiplexed photonic layer on CMOS).

#139924 - $15.00 USD Received 20 Dec 2010; revised 4 Feb 2011; accepted 1 Apr 2011; published 9 Jun 2011
(C) 2011 OSA